



## Cobalt and marine redox evolution



Elizabeth D. Swanner<sup>a,\*</sup>, Noah J. Planavsky<sup>b</sup>, Stefan V. Lalonde<sup>c</sup>, Leslie J. Robbins<sup>d</sup>,  
Andrey Bekker<sup>e</sup>, Olivier J. Rouxel<sup>f</sup>, Mak A. Saito<sup>g</sup>, Andreas Kappler<sup>a</sup>, Stephen  
J. Mojzsis<sup>h,i,j</sup>, Kurt O. Konhauser<sup>d</sup>

<sup>a</sup> Department of Geosciences, Eberhard-Karls University Tübingen, Sigwartstrasse 10, 72076 Tübingen, Germany

<sup>b</sup> Department of Geology and Geophysics, Yale University, New Haven, CT 06520, USA

<sup>c</sup> UMR 6538 Domaines Océaniques, European Institute for Marine Studies, Technopôle Brest-Iroise, 29280 Plouzané, France

<sup>d</sup> Department of Earth and Atmospheric Sciences, University of Alberta, Edmonton, Alberta, T6G 2E3, Canada

<sup>e</sup> Department of Geological Sciences, University of Manitoba, Winnipeg, Manitoba, R3T 2N2, Canada

<sup>f</sup> IFREMER, Centre de Brest, Technopôle Brest-Iroise, 29280 Plouzané, France

<sup>g</sup> Marine Chemistry and Geochemistry Department, Woods Hole Oceanographic Institution, Woods Hole, MA 02543, USA

<sup>h</sup> Laboratoire de Géologie de Lyon, Ecole Normale Supérieure de Lyon and Université Claude Bernard Lyon 1, CNRS UMR 5276, 2 rue Raphaël Dubois, 69622 Villeurbanne, France

<sup>i</sup> Hungarian Academy of Sciences, Institute for Geological and Geochemical Research, 45 Budaörsi Street, H-1112 Budapest, Hungary

<sup>j</sup> Department of Geological Sciences, University of Colorado, UCB 399, 2200 Colorado Avenue, Boulder, CO 80309-0399, USA

## ARTICLE INFO

## Article history:

Received 24 July 2013

Received in revised form 20 December 2013

Accepted 2 January 2014

Available online xxxx

Editor: G.M. Henderson

## Keywords:

cobalt

trace element proxies

ocean redox

shale

iron formation

pyrite

## ABSTRACT

Cobalt (Co) is a bio-essential trace element and limiting nutrient in some regions of the modern oceans. It has been proposed that Co was more abundant in poorly ventilated Precambrian oceans based on the greater utilization of Co by anaerobic microbes relative to plants and animals. However, there are few empirical or theoretical constraints on the history of seawater Co concentrations. Herein, we present a survey of authigenic Co in marine sediments (iron formations, authigenic pyrite and bulk euxinic shales) with the goal of tracking changes in the marine Co reservoir throughout Earth's history. We further provide an overview of the modern marine Co cycle, which we use as a platform to evaluate how changes in the redox state of Earth's surface were likely to have affected marine Co concentrations. Based on sedimentary Co contents and our understanding of marine Co sources and sinks, we propose that from ca. 2.8 to 1.8 Ga the large volume of hydrothermal fluids circulating through abundant submarine ultramafic rocks along with a predominantly anoxic ocean with a low capacity for Co burial resulted in a large dissolved marine Co reservoir. We tentatively propose that there was a decrease in marine Co concentrations after ca. 1.8 Ga resulting from waning hydrothermal Co sources and the expansion of sulfide Co burial flux. Changes in the Co reservoir due to deep-water ventilation in the Neoproterozoic, if they occurred, are not resolvable with the current dataset. Rather, Co enrichments in Phanerozoic euxinic shales deposited during ocean anoxic events (OAE) indicate Co mobilization from expanded anoxic sediments and enhanced hydrothermal sources. A new record of marine Co concentrations provides a platform from which we can reevaluate the role that environmental Co concentrations played in shaping biological Co utilization throughout Earth's history.

© 2014 Elsevier B.V. All rights reserved.

## 1. Introduction

The availability of bio-essential trace elements such as Fe, Mo, Zn, Co, Ni, and Cu underpins the emergence, long-term evolution, and activity of life on our planet. The record of trace element utilization imprinted in modern organisms is commonly thought to reflect metal availability in seawater when key metalloproteins

evolved (Dupont et al., 2006; Fraústo da Silva and Williams, 2001; Zerkle et al., 2005). The availability and removal of trace elements within aqueous habitats for life reflects the compositional evolution of the Earth's crust, but is also controlled by redox changes driven by metabolic innovation (Anbar, 2008). Temporal patterns in the concentrations and isotopic variations of trace elements in ancient sediments can serve as proxies for major changes in redox conditions in the oceans and atmosphere over geologic timescales (Anbar, 2008; Konhauser et al., 2009; Scott et al., 2008, 2012), and can provide a means to test the idea that environmental availability controlled the evolutionary history of metal utilization. However, empirical records of metal variation through time have

Abbreviations: Co, cobalt; Fe, iron; Mn, manganese; IF, iron formation; OMZ, oxygen minimum zone; OAE, oceanic anoxic event; MAR, mass accumulation rate.

\* Corresponding author. Tel.: +49 (0) 7071 29 73061.

E-mail address: elizabeth.swanner@ifg.uni-tuebingen.de (E.D. Swanner).

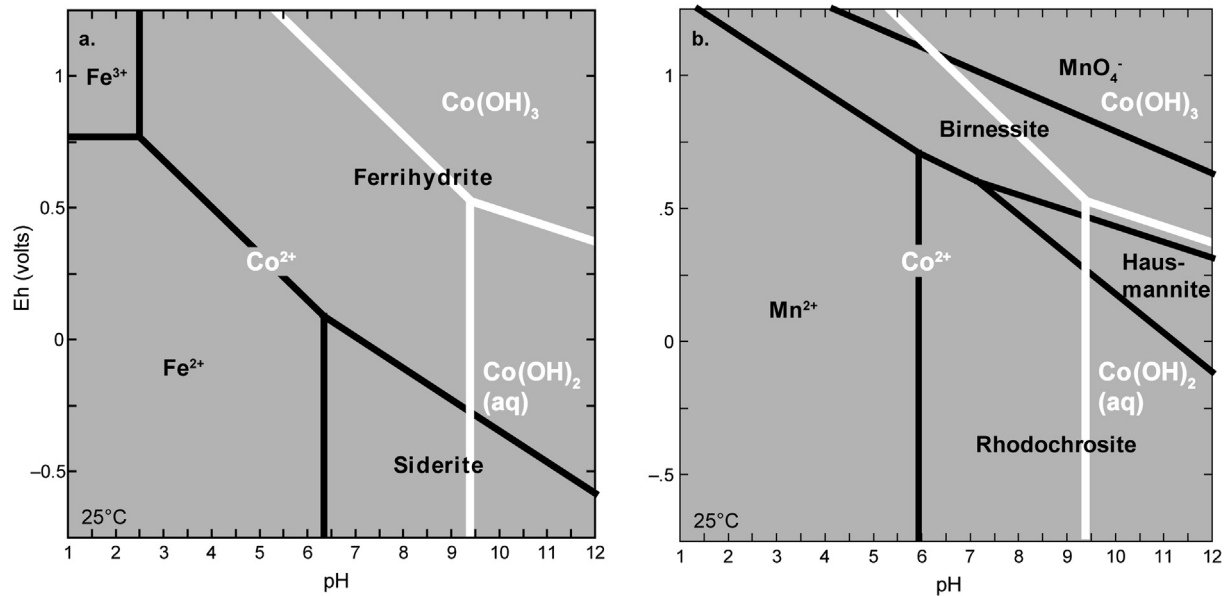


**Fig. 1.** a. Speciation diagram of Co (white) and Fe in varying Eh–pH conditions. Co<sup>2+</sup> is stable under marine Eh and pH conditions (i.e. 7–8) inferred for the Precambrian ocean. In the absence of carbonate, Fe<sup>2+</sup> is soluble. b. Speciation diagram of Co (white) and Mn, showing the similar redox potential for Mn(II) and Co(II) oxidation, which are both higher than that of Fe(II) oxidation.

only been described for a few trace elements. For some elements (e.g., Mo), the geochemical and biological records roughly converge on and support the interpretation of limited availability and biological utilization for early organisms (David and Alm, 2011; Scott et al., 2008). For other metals, the records do not match so well. For instance, Zn is an especially important yet relatively late adoption in eukaryotic metal-binding protein domains. As such, it was believed that Zn was relatively scarce in seawater until the Neoproterozoic when the oceans became fully oxygenated (Dupont et al., 2006). Yet, surprisingly, Zn abundance in the oceans appears to have been relatively constant throughout much of Earth's history (Scott et al., 2012), and Zn bioavailability may have been limited by the formation of soluble complexes with organics or sulfide (Robbins et al., 2013). Similarly, Ni concentrations were elevated in Archean seawater (Kamber, 2010; Konhauser et al., 2009), yet the proteomic record suggests increasing post-Archean biological Ni utilization (e.g. David and Alm, 2011). Genomic reconstructions support the early biological utilization of Co (David and Alm, 2011; Dupont et al., 2006), perhaps reflecting an ancient abundance of dissolved marine Co relative to the modern oceans. However, this model has not yet been tested against the geological record.

Cobalt is a bio-essential metal for life, forming amongst others, the central cobalt-corrin complex of cobalamin (vitamin B<sub>12</sub>). Eukaryotes use Co primarily as cobalamin in, for example, methionine synthesis. Bacteria and archaea additionally use cobalamin in enzymes for anaerobic metabolisms, including fermentation, dehalogenation, and one-carbon compound electron transfers (Banerjee and Ragsdale, 2003). Direct binding of Co also occurs in enzymes such as nitrile hydratase, used in amide metabolism. Cobalt can also substitute for Zn in carbonic anhydrase, an enzyme responsible for interconversion of CO<sub>2</sub> and bicarbonate in some phytoplankton, suggesting that marine Co availability is important in regulating the global carbon cycle (Morel et al., 1994).

Cobalt concentrations in modern seawater vary from 3 to 120 pM (Saito and Moffett, 2002), with variations dependent on interactions with other metals, biota and organic matter. Cobalt shows nutrient-like behavior with surface minimum concentrations due to biological uptake by phytoplankton (Saito et al., 2010; Saito and Moffett, 2002). Yet strong Co ligands complex nearly all of the dissolved Co in some oligotrophic waters (Noble et al., 2008;

Saito et al., 2004; Saito and Moffett, 2001; Saito et al., 2005), although some portion of this complexed Co pool is likely bioavailable (Saito et al., 2004; Saito and Moffett, 2001). In coastal and deep waters, Co behaves as a scavenged-type element (Moffett and Ho, 1996; Saito et al., 2004), becoming oxidized and adsorbed to Mn(III,IV) oxides as they precipitate (Murray and Dillard, 1979). Co scavenging is thought to be catalyzed by Mn(II)-oxidizing bacteria (Moffett and Ho, 1996; Murray et al., 2007).

Previous estimates of marine Co concentrations through Earth's history were based on thermodynamic considerations and assumptions regarding evolving marine redox and chemical composition (Saito et al., 2003), and did not consider how some key sources and sinks changed through time. Furthermore, equilibrium mineral precipitation models neglect kinetic control over precipitation. In this study, we use the sedimentary record of Co to track first-order changes in the marine Co reservoir through time, along with estimated magnitudes of the modern sources and sinks to infer the causes for Co reservoir change. We also suggest that the contents of Co of authigenic marine pyrite can be used as a proxy for marine Co concentrations.

## 2. Behavior of Co in marine environments

The formation of authigenic marine phases is subject to thermodynamic control, based on the abundance and speciation of ions, redox, and pH conditions. However, kinetically-driven scavenging reactions also influence the composition of marine precipitates. As a basis for the discussion below, Eh–pH diagrams detailing Co speciation were generated with the Act2 module of Geochemists' Workbench using the Minteq thermodynamic database from 2005. Cobalt(II) was set to 100 nM, Fe(II) and Mn(II) to 50 μM, bicarbonate to 5 mM, silica to 2.2 mM (saturation with amorphous silica; Konhauser et al., 2007) in seawater ionic strength; physical constraints were 25°C and 1 atmosphere ambient pressure. Cobalt does not form carbonate compounds, and Co(OH)<sub>3</sub> precipitates are only possible at very high Eh–pH conditions (Fig. 1). Cobalt(II) is oxidized to Co(III) in the same Eh–pH space where Mn(II) oxidation occurs, accounting for the oxidation of Co(II) and adsorption of Co(III) to precipitated Mn(III,IV) oxides (Murray and Dillard, 1979; Takahashi et al., 2007). Iron(II) is oxi-

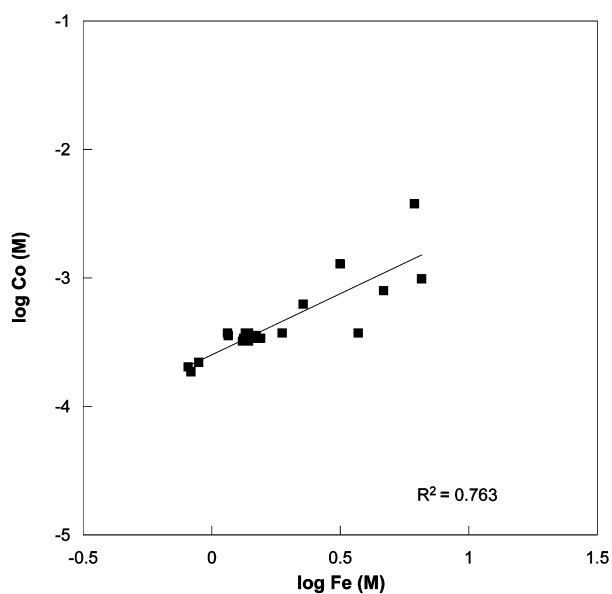


**Fig. 2.** Co-precipitation of Co with Fe (oxyhydr)oxides can be inferred based on a correlation coefficient of 0.763 from previously published data from hydrothermal sediments at the Endeavor Segment, Juan de Fuca Ridge (Hrshceva and Scott, 2007).

dized to Fe(III) at a lower redox potential than Co(II) and Mn(II) at marine pH ( $\sim 8$ ).

Adsorption of Co(II) and Co(III) to surface sites on Fe(III) (oxyhydr)oxides (Musić et al., 1979) and Mn(III,IV) oxides (Takahashi et al., 2007), respectively, is an important pathway for scavenging of Co under oxic conditions (Koschinsky and Hein, 2003; Stockdale et al., 2010; Takahashi et al., 2007). Soluble Co maxima occur below the  $O_2$ – $H_2S$  chemocline in modern euxinic basins in conjunction with both the soluble Fe and Mn peaks (Dryssen and Kremling, 1990; Öztürk, 1995; Viollier et al., 1995), which indicates that Co is released by reductive dissolution of both Mn(III,IV) oxides and Fe(III) (oxyhydr)oxides. Both poorly crystalline and crystalline Fe(III) (oxyhydr)oxide surfaces efficiently scavenge Co(II) in waters with pH above  $\sim 7$  (Gunnarsson et al., 2000; Musić et al., 1979; Dzombak and Morel, 1990), likely as bidentate inner-sphere complexes (Beak et al., 2011), while Co(III) is substituted for Mn in Mn(III/IV) oxides (Manceau et al., 1997). Correlation between Co and Fe in hydrothermal sediments collected from Endeavor Segment, Juan de Fuca (Fig. 2; data from Hrshceva and Scott, 2007) implies a common delivery path for both metals and is consistent with an Fe(III) (oxyhydr)oxide Co shuttle.

Sorption of Co(II) to ferrihydrite, likely the dominant Co scavenging pathway in Fe(II)-rich seawater (e.g. Konhauser et al., 2009), was investigated with MINTEQA3 using constants and site densities previously determined for ferrihydrite (Dzombak and Morel, 1990). Activities of dissolved components were corrected using the Davies equation, and modeling utilized 100 pM initial Co(II), 0.56M NaCl electrolyte to simulate seawater, and 1 g/L free ferrihydrite mineral (a constant concentration of surface sites during steady-state production of ferrihydrite). We compared Co sorption with and without Co ligands at modern (ca. 40 pM; Saito et al., 2004; Saito and Moffett, 2001) and high (400 pM) concentrations to investigate whether Co ligands prevent sorption of Co(II) to surface sites of ferrihydrite. The amount of Co(II) sorbed was unaffected at marine pH with 40 pM ligands, but Co(II) sorption to ferrihydrite was negligible when ligand concentrations were 400 pM (Fig. 3). We note that this model utilizes data for ligands specific to Co(II), but Co(III)-ligand complexes are likely extremely inert (Saito et al., 2005), and should further decrease the pool of Co available for metal sorption. We also did not examine the effects of inorganic species (e.g. Si), which can compete with metals for sur-

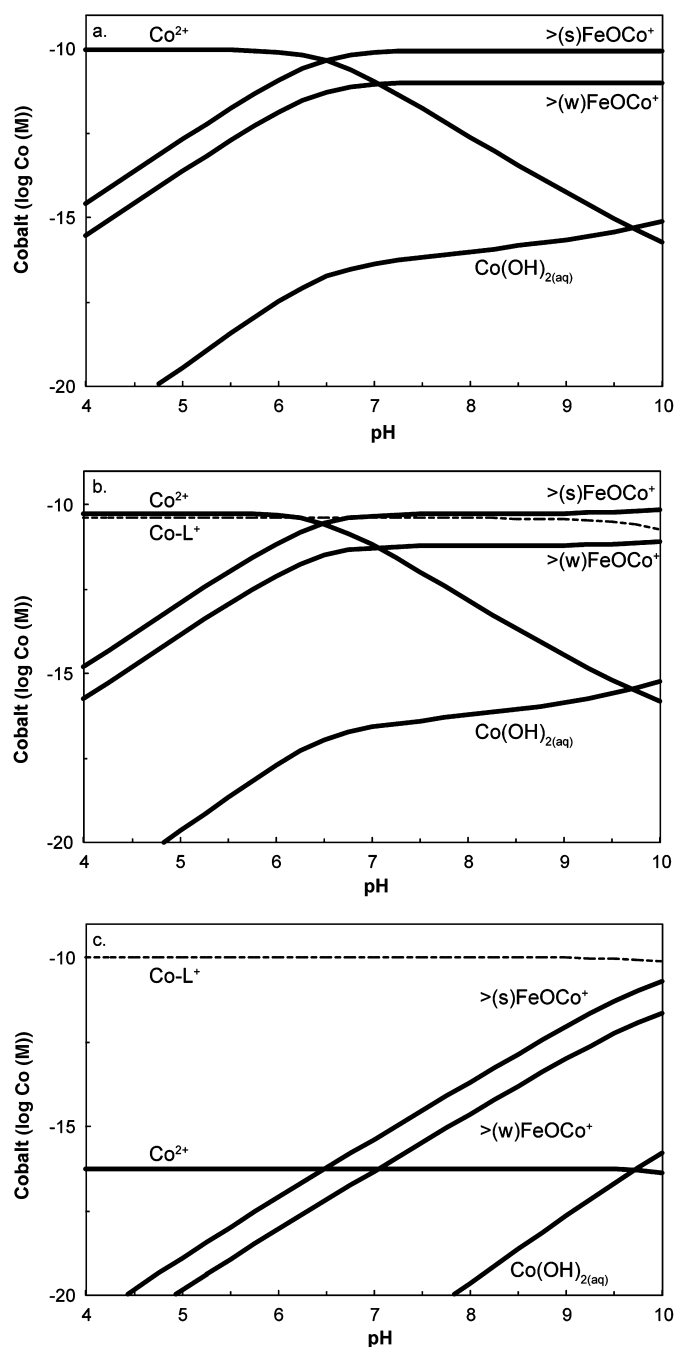


**Fig. 3.** Sorption of  $Co^{2+}$  to strong  $>(s)$  and weak  $>(w)$  surface sites on ferrihydrite in seawater when a. no organic Co-ligands are present, b. modern (40 pM) concentrations of organic ligands (dashed line) are present, and c. for an extreme case of 400 pM of organic ligands.

face binding sites on ferrihydrite (Konhauser et al., 2007, 2009). As illustrated by those studies, the presence of Si should lower the amount of metal bound for any given dissolved Co concentration.

In oligotrophic surface waters, Co concentrations are controlled by phytoplankton uptake and binding to organic ligands (Saito and Moffett, 2001, 2002) rather than by the scavenging reactions with Mn that occur in coastal and deep waters (Moffett and Ho, 1996). Cobalt concentrations in phytoplankton are similar to abundances of Cd and Cu and enriched by as much as  $10\times$  over Mo (Ho et al., 2003). Organic material can also sorb trace elements and transfer them to sediments (Broecker and Peng, 1982; Krauskopf, 1956), although this process is not as quantitatively significant for Co as

**Table 1**  
Modern cobalt budget.

Sources		
Riverine flux	$5.5 \times 10^{12}$	$\text{g kyr}^{-1}$
Hydrothermal flux	$1.3 \times 10^{11}$	$\text{g kyr}^{-1}$
Oceanic reservoir mass	$1.6 \times 10^{12}$	$\text{g}$
Residence time	0.28	$\text{kyr}$
Sinks		
Oxic MAR	2.3–5	$\mu\text{g Co cm}^{-2} \text{kyr}^{-1}$
Euxinic MAR	5	$\mu\text{g Co cm}^{-2} \text{kyr}^{-1}$

it is for other metals (e.g., Cd, Zn; Algeo and Maynard, 2004; Yee and Fein, 2003).

The formation of sulfide minerals governs the concentrations of Co in anoxic and sulfidic waters. Cobalt sulfide is more soluble than sulfides of some other biologically important elements (e.g. Cu, Zn; Saito et al., 2003), and dissolved Co concentrations below the chemocline of sulfidic waters can exceed average ocean concentrations by several orders of magnitude (Dryssen and Kremling, 1990; Viollier et al., 1995). Previous calculations suggested that the formation of Co-sulfide should scavenge dissolved Co from sulfidic waters (Dryssen and Kremling, 1990; Kremling, 1983), but little evidence exists for this particulate Co phase (Saito et al., 2003). Further, field observations show that some Co remains dissolved in sulfidic waters, while less soluble metals (e.g., Cu, Cd) are rapidly removed (Öztürk, 1995; Viollier et al., 1995). The exchange of the bisulfide ion with water molecules hydrating dissolved Co(II) is slower than with those hydrating Fe(II), likely contributing to the persistence of dissolved Co(II) in sulfidic waters (Morse and Luther, 1999). For most sulfidic marine systems, this means that while FeS is more soluble than CoS (from a thermodynamic point of view; e.g. Saito et al., 2003), FeS formation is kinetically favored, and Co is incorporated into FeS rather than precipitating as CoS (Huerta-Diaz and Morse, 1992; Morse and Arakaki, 1993).

The concentration of metals, including Co, in sulfidic waters is also buffered by the formation of soluble metal-sulfide complexes (Daskalakis and Helz, 1992), although this seems to be more important for metals such as Cd, Zn, and Cu that form stronger sulfide complexes. However, above 1  $\mu\text{M}$  total sulfide, soluble Co-sulfide complexes will reduce the dissolved Co(II) pool (Saito et al., 2003). Regardless of the initial phase of aqueous precipitate, Co ultimately substitutes into pyrite during sedimentary diagenesis (Huerta-Diaz and Morse, 1992; Stockdale et al., 2010).

### 3. Marine Co sources and sinks

The concentration of elements in seawater reflects a balance between delivery and removal of elements via precipitation and adsorption processes (e.g. Broecker, 1971; Krauskopf, 1956). To quantitatively interpret changes in the marine Co reservoir, as recorded by sediments deposited under different redox conditions, we detail below estimates of the fluxes of dissolved Co to seawater, and mass accumulation rates (MAR) for sediments deposited under oxic, anoxic and euxinic conditions (Table 1).

#### 3.1. Marine Co sources

The amount of Co present in the crust ultimately governs the amount of Co delivered to the oceans through fluid–rock interaction. Minerals with higher Fe, Mg, and Cr contents are also enriched in Co (Carr and Turekian, 1961), specifically olivine and pyroxene present in ultramafic rocks (Glassley and Piper, 1978). Dissolved Co is delivered to seawater via rivers and hydrothermal fluids that source Co predominantly from mafic and ultramafic

rocks. The estimated riverine flux of Co is  $5.5 \times 10^{12} \text{ g kyr}^{-1}$  (Table 1; Gaillardet et al., 2003). Cobalt fluxes from the continents were likely higher prior to 2.5 Ga due to their more mafic compositions, after which average Co concentrations in the continental crust dropped from 22 to 15 ppm (Condie, 1993). Dust can add dissolved Co to surface waters, but this process is likely to be minor and geographically and seasonally restricted (Shelley et al., 2012).

Although recent work has highlighted the role of hydrothermal fluids in supplying scavenged-type elements to the ocean reservoir (e.g. Fe; Saito et al., 2013; Tagliabue et al., 2010), initial measurements have found little evidence for Co fluxes from hydrothermal systems to seawater (Noble et al., 2012, 2008). However, hydrothermal fluids contain Co in concentrations often several orders of magnitude above average seawater (Metz and Trefry, 2000), implying that delivery of hydrothermal Co to open oceans is limited by efficient, near-field scavenging reactions in oxic seawater (German et al., 1991). Using the fluid flow volume through high- and low-temperature hydrothermal systems as estimated from the oceanic Mg budget by Elderfield and Schultz (1996), we calculated Co fluxes out of both types of systems as described by Reinhard et al. (2013). The Co anomaly for high-temperature systems utilized the difference between concentrations within the Plume vent on the Juan de Fuca Ridge ( $200 \text{ nmol kg}^{-1}$  at  $246^\circ\text{C}$ ) and bottom waters ( $0.02 \text{ nmol kg}^{-1}$ ; Metz and Trefry, 2000). The Co anomaly for low-temperature systems was based on Co data from site 1027 on the Juan de Fuca Ridge ( $0.7 \text{ nmol kg}^{-1}$  at  $64^\circ\text{C}$ ) relative to bottom waters ( $0.03 \text{ nmol kg}^{-1}$ ; Wheat et al., 2003). We estimate a total hydrothermal Co flux of  $1.2 \times 10^{11} \text{ g Co kyr}^{-1}$ ; 2.4% of the total Co flux (Table 1). We recognize that the net fluxes of most hydrothermally derived metals to the open ocean remain poorly constrained; metals released from hydrothermal vents are readily incorporated into sulfide or oxide precipitates within plumes, thereby diminishing dispersion. However, nanoparticulate sulfides or organic ligands may stabilize and transport trace elements away from vents (Sander and Koschinsky, 2011; Toner et al., 2009; Yucel et al., 2011), increasing trace element, and probably Co, fluxes to the global ocean. We therefore anticipate that global fluxes of Co from hydrothermal systems will be refined in the near future (e.g. GEOTRACES).

#### 3.2. Oxic sedimentary Co sinks

In sediments where oxygen penetrates at least 1 cm, authigenic Fe(III) (oxyhydr)oxides, Mn(III/IV) oxides and associated Co are permanently buried (Brumsack, 1989; Froelich et al., 1979). Any Fe(II) and Mn(II) released during dissimilatory microbial reduction is likely to be reoxidized and immobilized before diffusing out of sediments. Deposition of phytoplankton biomass may also add Co to oxic sediments (Saito et al., 2004). Regardless of the pathway for authigenic Co delivery to sediments, Co released during early diagenesis is immobilized by scavenging with Fe(III) (oxyhydr)oxides and Mn(III/IV) oxides. Cobalt fluxes to oxic continental margin and hydrothermal sediments are higher than those in the deep sea (Douglas and Adeney, 2000; Koschinsky and Hein, 2003), but these fluxes are not well-constrained. We use an estimate of  $2.3\text{--}5 \mu\text{g Co cm}^{-2} \text{kyr}^{-1}$  (Krishnaswami, 1976) from deep-sea pelagic sediments for an average authigenic oxic Co MAR.

#### 3.3. Euxinic sedimentary Co sinks

Modern sulfidic (sulfide in porewaters) or euxinic (sulfide in bottom waters) environments include basins where authigenic Fe(III) (oxyhydr)oxides and Mn(III/IV) oxides are reductively dissolved below the  $\text{O}_2\text{--H}_2\text{S}$  transition zone, releasing associated Co

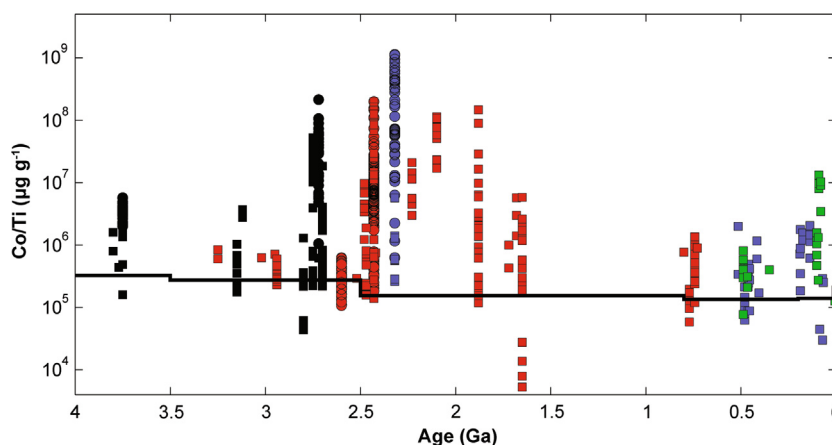


**Fig. 4.** The Co/Ti of IF (symbols) and of evolving continental crust (black line; [Condie, 1993](#)). Data points are from bulk (squares) and laser-ablation (circles) analyses of Precambrian Superior-type IF (red) and Algoma-type IF (black). Also included are Phanerozoic shallow-marine ironstones (blue) and hydrothermal and exhalative deposits (green). Data points with  $>0.5$  wt% Mn have been excluded from this compilation.

([Dryssen and Kremling, 1990](#); [Öztürk, 1995](#); [Viollier et al., 1995](#)). To estimate an euxinic Co MAR, we subtracted the average terrigenous Co/Al ratio ( $198 \mu\text{g g}^{-1}$ ) from the Co/Al ratio of euxinic sediments ( $204 \mu\text{g g}^{-1}$ ; within errors) from the perennially euxinic Cariaco basin near Venezuela ([Piper and Dean, 2002](#)). Utilizing an average sedimentation rate, density, and porosity for euxinic Cariaco sediments ([Lyons et al., 2003](#)), our estimated euxinic Co MAR is  $5 \mu\text{g Co cm}^{-2} \text{ kyr}^{-1}$  ([Table 1](#)). We acknowledge that there are large errors in this estimate, and higher euxinic Co MAR are observed in restricted basins ([Brumsack, 1989](#); [Hetzler et al., 2009](#)). Although Co is likely enriched above detrital levels in euxinic sediments, there is almost an order of magnitude lower enrichment than metals that form strong sulfide complexes (e.g., Mo), which can be enriched up to  $100\times$  above concentrations in oxic sediments ([Algeo and Maynard, 2004](#)). Cobalt MAR in euxinic sediments below open marine conditions ( $5 \mu\text{g Co cm}^{-2} \text{ kyr}^{-1}$ ) are similar to Co MAR in oxic marine sediments ( $2.3$  to  $5 \mu\text{g Co cm}^{-2} \text{ kyr}^{-1}$ ), in contrast to Mo (see [Scott et al., 2008](#)), demonstrating that expansion of euxinic sediments at the expense of oxic sediments, or vice versa, should not result in major changes to the Co reservoir.

#### 3.4. Anoxic sedimentary Co sinks

In anoxic marine sediments lacking dissolved sulfide, Fe(III) (oxyhydr)oxides and Mn(III/IV) oxides are subject to dissimilatory microbial reduction. Fluxes of Co(II) and Mn(II) have been observed out of sediments underlying oxygen- and sulfide-poor bottom water ([Brumsack, 1989](#); [Saito et al., 2004](#)), and plumes of dissolved Co mobilized from anoxic sediments have been observed over oxygen minimum zones (OMZs; [Noble et al., 2012](#)), demonstrating the mobility of Co under anoxic conditions. While remobilization under anoxic conditions is an important source of Co in some coastal environments, this process does not represent an exogenous supply of Co, and so we have not included reducing sediments as a source in flux estimates. Because Co is readily mobilized from anoxic sediments, there is no significant flux of Co to anoxic sediments, and Co in anoxic sediments solely reflects what is added with detrital minerals ([Brumsack, 1989](#); [van der Weijden et al., 2006](#)). Thus, a decrease in the extent of anoxic sediments at the expense of oxic or euxinic sediments will decrease the size of dissolved Co reservoir, while expansion of anoxic sediments should increase the size of the reservoir.

Generally speaking, sediments deposited under an anoxic but non-sulfidic water column, which are often referred to as ferruginous sediments, are also unlikely to permanently remove Co. Rare

in the modern but common in the Precambrian, ferruginous sediments are characterized by overlying water column with anoxic conditions with Fe(II) as the main redox buffer ([Planavsky et al., 2011](#)). These redox conditions also allowed for the deposition of iron formations (IF), which are likely to be a significant Co sink ([Fig. 4](#)). However, IFs reflect stabilization of Fe(III) (oxyhydr)oxides under anoxic conditions where there was anomalously high local Fe(III) fluxes. Furthermore, most oxide facies IF are found in deep water settings, and oxides are preserved due to a lack of sufficient organic carbon to drive complete Fe(III) reduction ([Konhauser et al., 2005](#)). Therefore, IF likely have higher capacities for Co burial (with authigenic Fe(III) (oxyhydr)oxides) than modern anoxic sediments, but IFs represent a small fraction of overall marine ferruginous settings.

#### 4. Archives of marine Co concentrations

We propose that sedimentary Co concentrations can serve as an archive of marine Co concentrations. We use this premise to evaluate how key sources and sinks for Co have varied through time. This compilation also informs the evolution of marine redox conditions. We focus on two types of sedimentary archives: those in which Co was sequestered by authigenic Fe(III) (oxyhydr)oxides (IF database), or by iron sulfides (sedimentary pyrite and euxinic shale databases).

##### 4.1. Iron formations as a Co archive

Iron(III) (oxyhydr)oxides, generally thought to be the precursor phases to most IF, have extremely large and reactive surfaces that extensively adsorb cations, including Co(II), at marine pH ([Dzombak and Morel, 1990](#)). Therefore, we propose that the record of authigenic Co enrichment in IF can be used to evaluate large-scale changes in marine Co concentrations through time. Similar chemical principles justified using Ni, P, and Zn enrichments in IF to track changes in seawater concentrations of these elements ([Konhauser et al., 2009](#); [Planavsky et al., 2010](#); [Robbins et al., 2013](#)). Precambrian IF are chemical precipitates with minor detrital input. Authigenic, but diagenetically and metamorphically altered, Fe-rich (hematite, magnetite, siderite) and Si-rich (quartz) phases dominate the mineralogy of IF, and so their trace element composition is often inferred to reflect input of these elements from authigenic vs. detrital phases. Post-depositional alteration of the primary trace element seawater signatures is generally minimal unless IF have experienced hydrothermal alteration or near surface weathering ([Bau and Moeller, 1993](#)).

Historically, Precambrian IF are divided into Algoma-type, which have a spatially limited extent and formed in proximity to volcanic and hydrothermal settings, and Superior-type, which are more extensive and where deposited under marine conditions on a continental shelf or an isolated basin. Both deposits are represented in our dataset and we assign each IF as being Algoma- or Superior-type for simplicity; in reality there is a gradation between these IF types (see Bekker et al., 2010). Large, basin-scale IF deposition experienced a hiatus in the Middle Proterozoic, and a return to IF deposition in the Neoproterozoic was followed by permanent cessation of IF deposition. The lack of IF in intervening intervals is evident in our compilation. We further utilize exhalite deposits and oolitic ironstones to extend the record of Co burial with authigenic Fe oxide facies into the Phanerozoic.

We utilize an expanded dataset of Konhauser et al. (2011, 2009), comprising published values as well as new data acquired by bulk analysis and *in situ* LA-ICP-MS. Supplementary Table 1 reports Co, Al, Ti, Fe, Mn, and S concentrations (where available) for the 1353 Co data points used in this study. The supplementary information also includes references for the published data and the descriptions of iron formations analyzed in this study.

#### 4.2. Pyrite as a Co archive

The partitioning of Co into iron sulfide phases is dependent on Co and Fe concentrations, but importantly for our purposes, it appears to be largely independent of the amount of hydrogen sulfide (Morse and Arakaki, 1993). In most sulfidic environments, dissolved Fe<sup>2+</sup> concentrations are near levels predicted from equilibrium with the amorphous Fe–S phase mackinawite (e.g. Helz et al., 2011). Finally, silicate phases react with sulfide 10<sup>8</sup> × more slowly than Fe(III) (oxyhydr)oxide minerals (Canfield et al., 1992), so Co in detrital minerals should not contribute to Co concentrations in pyrite. Therefore, it is reasonable to assume that the degree of authigenic Co enrichment in sediments deposited below euxinic waters should, to a first order, reflect the dissolved Co concentrations in the water column.

In order to use trace element concentrations within pyrite as proxies for seawater concentrations during sediment deposition, it is essential that (1) pyrites formed within the sediments that host them, and (2) the metal inventory of pyrite was not overprinted by secondary alteration processes. In the absence of free oxygen in the Archean atmosphere, detrital pyrite was delivered to marine sediments (Rasmussen and Buick, 1999). Therefore, only sulfides with early diagenetic textures (e.g. nodules or disseminated grains) from shales with abundant organic carbon and sulfur and were included in this study (Rouxel et al., 2005), although not all of the sediments included in this study have been definitively demonstrated to have been deposited under euxinic conditions. Post-depositional disturbances to metal content were screened by selecting samples with no obvious sign of alteration (Rouxel et al., 2005, 2006).

Individual pyrite grains from black shales were digested and trace element data were acquired by Thermo Element2 HR-ICP-MS at Woods Hole Oceanographic Institution as described by Rouxel et al. (2005). A basic description of each sample, as well as the geological setting and age constrains for the host rock, are reported by Rouxel et al. (2005). Previously unreported samples include Devonian-age black shales from the Illinois basin, pyrite nodules from the ca. 1.8 Ga Gunflint Formation of Kakabeca Falls in Ontario, Canada, and pyrite from the ca. 2.7 Ga Manjeri Formation of the Belingwe Belt, Zimbabwe. Cobalt concentrations are reported in Supplementary Table 2. Trace element compositions of pyrite from modern anoxic sediments are taken from Huerta-Diaz and Morse (1992) and reference cited therein.

**Table 2**

Statistical differences between cobalt concentrations in sediments by age bin.

<i>Iron formations</i>			
Age bin	Mean Co/Ti ( $\mu\text{g g}^{-1}$ )	* / SD	<i>p-value</i> *
$\geq 2.80$ Ga	79.85	1.72	
2.75 to 1.88 Ga	150.57	2.67	<0.0001
$\leq 1.72$ Ga	62.25	1.84	<0.0001
<i>Euxinic shale pyrite</i>			
Age bin	Mean Co (ppm)	* / SD	<i>p-value</i> *
2.80 to 1.84 Ga	7.34	1.77	
1.80 to 0.30 Ga	3.87	1.96	<0.0001
<i>Euxinic shale</i>			
Age bin	Mean Co/Al ( $\mu\text{g g}^{-1}$ )	* / SD	<i>p-value</i> *
$\geq 0.695$ Ga	11.51	1.73	
$\leq 0.531$ Ga	9.33	1.97	0.0842

\* *p-values* refer to comparison between the age bin indicated and the preceding age bin.

#### 4.3. Bulk euxinic shales as a Co archive

Cobalt is enriched in sediments deposited under euxinic conditions (Algeo and Maynard, 2004), and the shales used in this study have Mo contents >25 ppm, consistent with euxinia (Scott and Lyons, 2012). Authigenic Co was distinguished from detrital Co via normalization to a conservative element, in this case Al. This approach is justified as the Co/Al ratio of fine-grained material derived from continents has varied little through time (Condie, 1993), and is similar amongst several compilations (Condie, 1993; Kamber et al., 2005; Wedephol, 1971). The Co and Al values for euxinic sediments used in this study have all been previously published (see Supplementary references). Because it is not always straightforward to distinguish detrital from authigenic trace elements in shales (e.g. Van der Weijden, 2002), we emphasize that the IF and pyrite datasets are likely to be the most robust indicators of the marine reservoir.

#### 4.4. Statistical analysis of Co datasets

When grouped by ages that correspond to global events (described below), Co concentrations were log-normally distributed. The statistical differences between average time-binned values were compared using an unpaired t-test of log concentration values. The *p* values for these comparisons are reported in Table 2. The mean and one standard deviation (SD) of log concentration values were then back-transformed to concentration values, and these are reported as mean ( $\mu\text{g g}^{-1}$ ) / SD in accordance with the multiplicative nature of a log-normal distribution (Limpert et al., 2001).

### 5. Evolution of the marine Co reservoir

#### 5.1. Reconstructing changes in Co sources and sinks through Earth history

The datasets of Co in IF, pyrite and shale reveal time-resolved patterns in the delivery of Co to marine sediments, and thereby indicate first-order changes to the marine Co reservoir through time (Fig. 4). The average Co/Ti ( $\mu\text{g g}^{-1}$ ) of IF  $\geq 2.80$  Ga (79.85 / 1.72) are significantly lower than IF deposited between 2.75 to 1.88 Ga (150.57 / 2.67). Average values then significantly drop in IF, exhalite, and oolitic ironstones deposited between 1.72 Ga and modern times (62.25 / 1.84; Table 2), despite that exhalites are prime

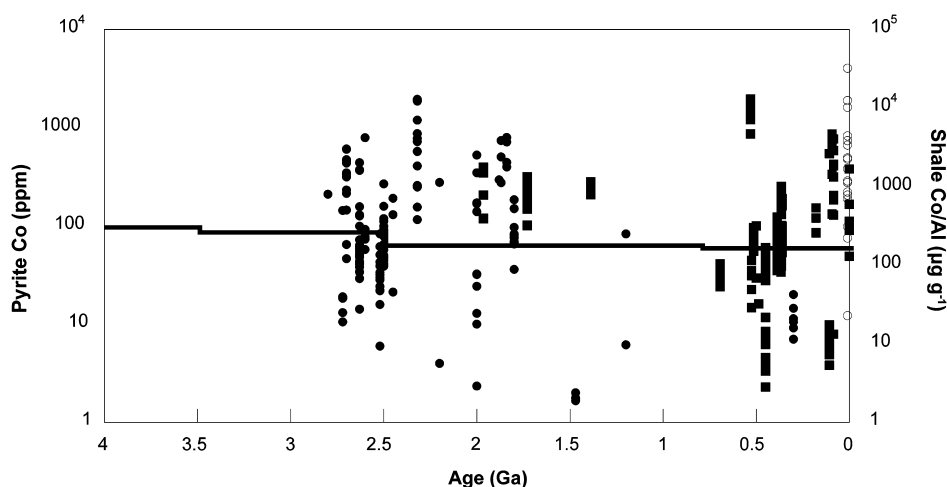


**Fig. 5.** Cobalt concentrations in pyrite (circles) from modern (open) and ancient (filled) euxinic shales, and bulk euxinic shales (squares). For reference, the crustal evolution trend (solid line) is included, based on the Restoration Model of [Condie \(1993\)](#). Modern pyrite Co concentrations from coastal sediments reflect high concentrations of trace metals delivered from rivers and petroleum reservoirs ([Huerta-Diaz and Morse, 1992](#)).

records of locally derived hydrothermal Co. There is also a significant difference between the average concentrations of Co (ppm) in pyrites from shales deposited between 2.8 and 1.84 Ga ( $7.34 \cdot / 1.77$ ) and those deposited from 1.8 to 0.3 Ga ( $3.87 \cdot / 1.96$ ; [Table 2](#)), signifying a concordance of the IF and shale pyrite Co records, and likely global-scale trends in marine Co concentrations.

Higher seawater Co concentrations in the interval between 2.8 and 1.84 Ga reflect pervasive anoxia and a higher hydrothermal Co flux to the marine reservoir during the emplacement of oceanic crust, likely due in part to several mantle plume events at this time ([Barley et al., 2005](#); [Rasmussen et al., 2012](#)). These events also likely supplied the Fe for major IF deposited from 2.5 to 2.4 Ga, and again between 1.9 and 1.8 Ga ([Barley et al., 1997](#); [Rasmussen et al., 2012](#)). In hydrothermal systems, the supply of Co tracks that of Fe ([Douville et al., 2002](#)) because the solubility of both elements is enhanced at higher temperature and  $\text{Cl}^-$  concentrations ([Metz and Trefry, 2000](#)). Archean-aged hydrothermal systems are thought to have experienced higher heat flow, enhancing the supply of Fe ([Isley, 1995](#)), and likely Co to seawater. Higher Co concentrations from Archean hydrothermal fluids are also more likely due to the prevalence of ultramafic oceanic crust ([Arndt, 1983](#)). Compositional control on Co concentrations in hydrothermal fluids is indicated in the ultramafic Rainbow vent field on the Mid-Atlantic Ridge, where Co concentrations reach up to  $13 \mu\text{M}$  Co ([Douville et al., 2002](#)), an enrichment of at least  $10^5$  above seawater concentrations. Persistent anoxia would have allowed the dispersion of dissolved Co plumes without trapping near source by oxidative scavenging ([Noble et al., 2012](#)). These factors indicate an increased proportion of hydrothermal Co fluxes relative to continental Co fluxes in comparison to modern Co inputs ([Table 1](#)).

The Co concentrations in younger than 1.84 Ga IF are comparable to those prior to 2.8 Ga ([Table 2](#)), potentially indicating that weathering of mafic to ultramafic Neoproterozoic continental crust is not an essential aspect of the large enrichments. This is in contrast to Ni, whose supply to oceans from weathering of emergent oceanic plateaus waned after 2.7–2.6 Ga ([Kamber, 2010](#); [Konhauser et al., 2009](#)). Although Co and Ni have generally similar low-temperature geochemical behavior, they are decoupled during high-temperature hydrothermal alteration. Nickel is not as efficiently leached as Co, resulting in low hydrothermal Ni fluxes ([Douville et al., 2002](#)). Furthermore, Co-chloride complexes are more stable than Cu-, and, probably, Ni-chloride complexes, resulting in higher Co solubility at low temperatures ([Metz and Trefry, 2000](#)). The increase in marine sediment Co concentrations after

ca. 2.8 Ga may be driven by changes in the riverine flux of Co from the continents due to increased, permanent, subaerial exposure. Other authors have suggested the emergence of continents between 2.9 and 2.7 Ga (e.g. [Pons et al., 2013](#) and references within). However, the crustal growth rate slows and Co concentrations drop at 2.5 Ga, from 22–25 ppm ([Condie, 1993](#)), in the midst of the highest sedimentary Co concentrations ([Figs. 4 and 5](#)).

We propose that the drop in Co concentrations in marine sediments that occurs after 1.84 Ga reflects a decrease in intense, plume-related hydrothermal activity ([Rasmussen et al., 2012](#)). As supply of hydrothermal Fe and deposition of massive IF waned in the late Paleoproterozoic, so too did the hydrothermal Co flux, shifting towards modern conditions in which continentally-derived Co dominates Co influx ([Table 1](#)). Hydrothermal supply to the oceans reached modern levels by 0.7–0.8 Ga ([Derry and Jacobsen, 1988](#)), with episodic larger mantle inputs re-occurring throughout the Proterozoic and Phanerozoic ([Peng et al., 2011](#); [Veizer et al., 1983](#)). Additional Middle Proterozoic samples would be needed to test whether later mantle plume events resulted in a return to globally high marine Co concentrations.

The drop in seawater Co concentrations after 1.88 Ga occurs at a time when the extent of euxinic environments in the oceans increased ([Poulton et al., 2004](#)) at the expense of ferruginous sediments. Without well-constrained depositional rates for IF, it is impossible to estimate Co MAR from ferruginous settings, although our IF dataset attests to the fact that Co is effectively buried under ferruginous conditions. Nevertheless, given that IFs are rare marine sediments, the contribution of ferruginous sediments to overall Co removal in the oceans was likely low. Further, as stressed above, the Co sink associated with ferruginous settings will be lower than for oxic sediments; although Fe(III) (oxyhydr)oxides sorb Co, Mn(III/IV) oxides, which form at higher Eh, are much more effective at scavenging Co from seawater ([Stockdale et al., 2010](#)). Therefore, expansion of euxinic settings to less than 10% of seafloor area in the Middle Proterozoic ([Reinhard et al., 2013](#)), are unlikely to explain the drop in the Co reservoir size (cf. [Saito et al., 2003](#)) without invoking a waning hydrothermal Co source. Significant areal expansion of oxic and euxinic sediments might explain the drop in the Co reservoir, but oxic conditions suitable for Co scavenging were likely confined to Middle Proterozoic surface waters ([Poulton et al., 2004](#)), and sediments deposited under oxic conditions were of limited extent ([Reinhard et al., 2013](#)).

The logarithmic range of Co concentrations in sediments, even those from the same formation, is a phenomenon that has been observed for other trace elements (e.g. Zn; Robbins et al., 2013; Scott et al., 2012). This variability is likely primary, based on similar phenomena in modern authigenic sediments (Figs. 2 and 4). For Co, this may reflect temporal variability in marine Co concentrations, which is expected because Co is a non-conservative element within the oceans and has an extremely short residence time in seawater, 280 yr by our estimate (Table 1; 40–120 yr; Saito and Moffett, 2002). Due to its short residence time, marine Co concentrations respond quickly to perturbations in sources or sinks, such as the development of OMZ that fluctuate on decadal time scales (Noble et al., 2012; Stramma et al., 2008). The highest IF Co/Ti (nearly 160,000  $\mu\text{g g}^{-1}$ ) and pyrite Co (nearly 2000 ppm) are found in the 2.32 Ga Timeball Hill Formation and the underlying Rooihooft formations. Post-depositional hydrothermal overprint is likely not responsible for elevated Co concentrations because they do not correspond to high Pb or Cu, concentrations (data not shown), which would suggest mineralization. Some of this variation may be primary, and representative of temporally or spatially variable Co concentrations within the basin. However, some variability could be tied to re-distribution between Fe-phases during diagenesis. Despite these variations, the robust statistical differences in time-binned averages (Table 2) validate that shifts in sedimentary Co map onto global events, and hence, indicate reservoir changes.

Although there are no significant changes in the average Co concentrations from Middle Proterozoic to Phanerozoic in any of the sedimentary records (Table 2), there is significant variability in Phanerozoic euxinic shales (Fig. 5), many of which were deposited during ocean anoxic events (OAE), which reflect transient rather than pervasive anoxic conditions. The average Co/Al ratios from euxinic black shales deposited during the Cretaceous OAE-2A at Demerara Rise are  $\sim 2\times$  larger than euxinic sediments deposited before or after (their Fig. 9; Hertz et al., 2009). This is dramatically different from other redox-sensitive metals such as Mo and V, whose restricted supply was exhausted during the OAE, leading to depletions of Mo and V during the peak of the OAE relative to sediments deposited before and after. Cobalt is mobilized from anoxic sediments (Noble et al., 2012), and therefore increased Co burial in euxinic sediments might reflect this greater reservoir during anoxic events, and in fact be a proxy for low-oxygen conditions (Saito et al., 2010). OAE Co enrichments may also be linked to, or augmented by a hydrothermal Co pulse (e.g. Brumsack, 2006). Importantly, there is independent evidence for increased hydrothermal input from a sharp shift toward less radiogenic (hydrothermally-derived) initial Os isotope values during the onset of the OAE (Turgeon and Creaser, 2008). Furthermore, other authors have also documented sedimentary Co increases during OAE intervals linked to hydrothermal activity (Orth et al., 1993; Snow et al., 2005). Therefore, the OAE Co records are consistent with the notions developed above that anoxia and hydrothermal activity play a critical role in the global marine Co cycle, and that marine Co concentrations respond on shorter timescales than conservative elements such as Mo.

Surprisingly, we find little evidence for a change in the marine Co reservoir with the deep ocean oxygenation, potentially beginning as early as 635 Ma (Sahoo et al., 2012). The average Co/Al ( $\mu\text{g g}^{-1}$ ) for Proterozoic euxinic shales (11.51  $\cdot$  / 1.73) is not significantly different from Phanerozoic-aged shales (9.33  $\cdot$  / 1.97), although we emphasize that Phanerozoic shales are dominated by OAE samples, and likely reflect transient anoxia. There is also no statistical support for changes in IF or shale pyrite Co concentrations during similar time intervals (data not shown). We note however, that a paucity of datapoints from the Middle Proterozoic for all three databases hinders interpretation of changes to the Co

reservoir with deep ocean oxygenation. The highest Phanerozoic Co concentrations occur in exhalites, which demonstrate that near-source scavenging reactions prevent hydrothermal Co dispersal under oxic conditions, and therefore Phanerozoic exhalites likely reflect only local Co concentrations. Non-OAE euxinic shale pyrites would likely best track changes in the Co reservoir associated with ocean oxygenation. Because expanding oxic sediments at the expense of anoxic should enhance Co removal, and Neoproterozoic hydrothermal activity is likely similar to modern (Derry and Jacobson, 1988), ocean ventilation should have further decreased the Co reservoir size.

## 5.2. Marine cobalt reservoir size and biological evolution

Our empirical record of the marine Co reservoir affords an opportunity to discuss hypotheses of Co utilization in biology, and to consider how Co-utilization in aquatic organisms fit to these hypotheses. The biological utilization of metalloproteins may reflect the availability of elements in the environment in which the protein first appeared (e.g. Nisbet and Fowler, 1996). Genomic analyses of all three domains of life indicate that Co-binding proteins originated after 3.3 Ga (David and Alm, 2011). Given the uncertainties in this age stated by the authors ( $>250$  My), it is feasible that origin of many Co-binding proteins coincides with the enhanced marine Co availability we observe after 2.8 Ga, generally supporting the availability hypothesis. However, Co is chemically suited to catalyze reactions involving hydrogen rather than oxygen (Fraústo da Silva and Williams, 2001), and any preferential Co utilization by early organisms may simply reflect the abundance of reduced energy sources such as methane, carbon monoxide, and hydrogen on the early Earth (Zerle et al., 2005). Because higher Co availability is linked to periods in Earth's history when the oceans were anoxic, had on average lower Co burial rates, higher Co mobility, and probably longer Co residence times, environmental availability and catalytic suitability may both be reflected in the utilization of Co in organisms or early-evolved proteins.

Consistent with a greater utilization of Co by early organisms, bacteria and archaea have a greater number of genes that encode for Co-binding proteins (Zhang and Gladyshev, 2010), and their genomes encode a larger proportion of Co-binding proteins than eukarya (Dupont et al., 2006). In contrast, a lack of encoded Co-binding proteins in eukarya should indicate evolution predominantly after 1.8 Ga. This is broadly consistent with initial diversification of eukaryotes in the middle to late Proterozoic (Knoll et al., 2007). The persistence of the cobalamin-requiring gene *metH* in eukaryotic phytoplankton, involved in biosynthesis of the essential amino acid methionine, suggests that lower marine Co concentrations were not a sufficient selection pressure to drive loss of the *metH* gene in favor of a cobalamin-independent but less efficient gene (Bertrand et al., 2013), or that key Co-binding proteins were maintained and few new Co-binding proteins were acquired during genome expansion. Alternately, the persistence of *metH* in eukaryotic phytoplankton may reflect a later acquisition (Croft et al., 2005), and it often occurs in eukaryotic phytoplankton that already contained the cobalamin-independent gene (Helliwell et al., 2011). Thus, eukaryotic *metH* persistence may be related to its efficiency rather than Co availability.

Enzymes that directly bind Co rather than cobalamin also offer insight into how metal availability regulates enzyme utilization. Both diatoms and eukaryotic algae can substitute Co (or Cd) for Zn in the carbonic anhydrase enzyme that interconverts  $\text{CO}_2$  and bicarbonate when Zn concentrations are limiting (Morel et al., 1994; Saito and Goepfert, 2008). Such substitution may be a strategy for coastal algae to deal with intense metal drawdown during algal blooms (Saito and Goepfert, 2008), but also indicates that expression of metal-binding proteins encoded at the genomic level are



affected by temporally and spatially variable metal concentrations. The trends in Co sedimentary records presented here reflect geological control over element delivery and burial; short-term and spatial variability will therefore not be resolvable with our dataset. Furthermore, the amount of metal-binding protein expressed (i.e. the metallome) should fluctuate with physical and chemical conditions and the physiological state of the cell (Bertrand et al., 2013; Saito et al., 2011). Proteomics is therefore an important complement to genomic investigation of why utilization of metal-binding proteins persist, are lost or acquired as metal concentrations change.

Finally, although genomic utilization may reflect availability of metals during evolution, it can also indicate later adaptations to changing metal abundances. For instance marine cyanobacteria have an absolute requirement for Co that cannot be met by other metals (Saito et al., 2002; Sunda and Huntsman, 1995), which may reflect evolution in largely anoxic or sulfidic oceans with greater Co availability (Saito et al., 2003), yet thrive in the oxic oceans where Co concentrations are often less than 40 pM. Cobalt utilization may have persisted in cyanobacteria as Co availability declined due to the acquisition of Co-binding ligands (Saito and Moffett, 2001; Saito et al., 2005). The hypothesis that availability dictates utilization implies that the earliest life lacked strategies for acquisition of metals (Nisbet and Fowler, 1996). However, it is clear that modern organisms possess strategies to deal with limitation. Thus, the evolutionary history of metal-acquisition genes may be an important consideration when comparing metal availability to biological utilization, and many of these proteins are still being identified (Zhang and Gladyshev, 2010).

## 6. Conclusions

Trace elements are proxies for tracking marine redox evolution, but most studies have focused on metals that partition strongly into anoxic or sulfidic sediments (e.g., Mo). For Co, and Fe and Mn, which have short residence times in the modern ocean, marine concentrations respond dynamically to changes in delivery and removal. High seawater Co concentrations from ~2.8–1.84 Ga, recorded by IF and authigenic pyrites, resulted from widespread anoxia and enhanced hydrothermal activity and are probably linked to Fe fluxes that resulted in the deposition of IF. The marine Co reservoir decreased after ~1.84 Ga due to waning hydrothermal Co delivery. The expansion of euxinic sediments at the expense of anoxic sediments, which are a negligible sink for Co, may have also contributed to the Middle Proterozoic Co reservoir decrease. Variability of Phanerozoic IF and euxinic shale Co concentrations are linked to localized hydrothermal activity and/or transient anoxic conditions, and as such obscure any global changes in the marine Co reservoir associated with deep-water oxidation. Our study of the concentrations of Co in marine sediments through time reveals a more nuanced view of the marine Co reservoir through Earth's history than is possible with theoretical models based on thermodynamic equilibrium (e.g. Saito et al., 2003). This emerging view of the evolution of the marine Co reservoir through time provides a framework for interpreting Co availability influenced the acquisition and utilization of Co in biology.

## Acknowledgements

EDS acknowledges support of the National Science Foundation (NSF) IRFP and a Deutsche Forschungsgemeinschaft grant (KA 1736/24-1). NJP acknowledges support of the NSF EAR-PF and NSF ELT program. SVL gratefully acknowledges postdoctoral fellowship support from NSERC and LabEXMER. Discovery Grants and CGS-M from NSERC supported KOK, AB, and LJR, respectively. OR received support from Europe Mer and IFREMER. MAS was supported by

the Gordon and Betty Moore Foundation and the NSF Chemical Oceanography program. SJM was supported by the NASA Exobiology Program, NASA's Astrobiology Institute Fund for International Cooperation, the University of Colorado Center for Astrobiology, J.W. Fulbright Foundation, University of Colorado's Office of the Vice Chancellor for Research, and a sabbatical stay at the Centre de Recherches Pétrographiques et Géochimiques (CRPG-Nancy). This manuscript benefited from helpful discussions with Chris Reinhard and Martin Wille.

## Appendix A. Supplementary material

Supplementary material related to this article can be found online at <http://dx.doi.org/10.1016/j.epsl.2014.01.001>.

## References

- Algeo, T.J., Maynard, J.B., 2004. Trace-element behavior and redox facies in core shales of Upper Pennsylvanian Kansas-type cyclothems. *Chem. Geol.* 206, 289–318.
- Anbar, A.D., 2008. Elements and evolution. *Science* 322, 1481–1483.
- Arndt, N.T., 1983. Role of a thin, komatiite-rich oceanic crust in the Archean plate-tectonic process. *Geology* 11, 372–375.
- Banerjee, R., Ragsdale, S.W., 2003. The many faces of vitamin B12: catalysis by cobalamin-dependent enzymes. *Annu. Rev. Biochem.* 72, 209–247.
- Barley, M.E., Pickard, A.L., Sylvester, P.J., 1997. Emplacement of a large igneous province as a possible cause of banded iron formation 2.45 billion years ago. *Nature* 385, 55–58.
- Barley, M.E., Bekker, A., Krapež, B., 2005. Late Archean to Early Paleoproterozoic global tectonics, environmental change and the rise of atmospheric oxygen. *Earth Planet. Sci. Lett.* 238, 156–171.
- Bau, M., Moeller, P., 1993. Rare earth element systematics of the chemically precipitated component in Early Precambrian iron formations and the evolution of the terrestrial atmosphere–hydrosphere–lithosphere system. *Geochim. Cosmochim. Acta* 57, 2239–2249.
- Beak, D.G., Kirby, J.K., Hettiarachchi, G.M., Wendling, L.A., McLaughlin, M.J., Khatiwada, R., 2011. Cobalt distribution and speciation: effect of aging, intermittent submergence, in situ rice roots. *J. Environ. Qual.* 40, 679–695.
- Bekker, A., Slack, J.F., Planavsky, N., Krapež, B., Hofmann, A., Konhauser, K.O., Rouxel, O.J., 2010. Iron formation: the sedimentary product of a complex interplay among mantle, tectonic, oceanic, and biospheric processes. *Econ. Geol.* 105, 467–508.
- Bertrand, E.M., Moran, D.M., McIlvin, M.R., Hoffman, J.M., Allen, A.E., Saito, M.A., 2013. Methionine synthase interreplacement in diatom cultures and communities: Implications for the persistence of B12 use by eukaryotic phytoplankton. *Limnol. Oceanogr.* 58, 1431–1450.
- Broecker, W.S., 1971. A kinetic model for the chemical composition of sea water. *Quat. Res.* 1, 188–207.
- Broecker, W.S., Peng, T.-H., 1982. Tracers in the Sea. Lamont–Doherty Geological Observatory, Columbia University, Palisades, New York.
- Brumsack, H.-J., 1989. Geochemistry of recent TOC-rich sediments from the Gulf of California and the Black Sea. *Geol. Rundsch.* 78, 851–882.
- Brumsack, H.-J., 2006. The trace metal content of recent organic carbon-rich sediments: Implications for Cretaceous black shale formation. *Palaeogeogr. Palaeoclimatol. Palaeoecol.* 232, 344–361.
- Canfield, D.E., Raiswell, R., Bottrell, S., 1992. The reactivity of sedimentary iron minerals toward sulfide. *Am. J. Sci.* 292, 659–683.
- Carr, M.H., Turekian, K.K., 1961. The geochemistry of cobalt. *Geochim. Cosmochim. Acta* 23, 9–60.
- Condie, K.C., 1993. Chemical composition and evolution of the upper continental crust: Contrasting results from surface samples and shales. *Chem. Geol.* 104, 1–37.
- Croft, M.T., Lawrence, A.D., Raux-Deery, E., Warren, M.J., Smith, A.G., 2005. Algae acquire vitamin B12 through a symbiotic relationship with bacteria. *Nature* 438, 90–93.
- Daskalakis, K.D., Helz, G.R., 1992. Solubility of CdS (Greenockite) in sulfidic waters at 25 °C. *Environ. Sci. Technol.* 26, 2462–2468.
- David, L.A., Alm, E.J., 2011. Rapid evolutionary innovation during an Archean genetic expansion. *Nature* 469, 93–96.
- Dery, L.A., Jacobsen, S.B., 1988. The Nd and Sr isotopic evolution of Proterozoic seawater. *Geophys. Res. Lett.* 15, 397–400.
- Douglas, G.B., Adeney, J.A., 2000. Diagenetic cycling of trace elements in the bottom sediments of the Swan River Estuary, Western Australia. *Appl. Geochem.* 15, 551–566.
- Douville, E., Charlou, J.L., Oelkers, E.H., Bienvu, P., Jove Colon, C.F., Donval, J.P., Fouquet, Y., Prieur, D., Appriou, P., 2002. The rainbow vent fluids (36° 14' N, MAR): the influence of ultramafic rocks and phase separation on trace metal content in Mid-Atlantic Ridge hydrothermal fluids. *Chem. Geol.* 184, 37–48.

- Dryssen, D., Kremling, K., 1990. Increasing hydrogen sulfide concentration and trace metal behavior in the anoxic Baltic waters. *Mar. Chem.* 30, 193–204.
- Dupont, C.L., Yang, S., Palenik, B., Bourne, P.E., 2006. Modern proteomes contain putative imprints of ancient shifts in trace metal geochemistry. *Proc. Natl. Acad. Sci. USA* 103, 17822–17827.
- Dzombak, D.A., Morel, F.M.M., 1990. *Surface Complexation Modeling: Hydrous Ferric Oxide*. John Wiley & Sons, Inc.
- Elderfield, H., Schultz, A., 1996. Mid-ocean ridge hydrothermal fluxes and the chemical composition of the ocean. *Annu. Rev. Earth Planet. Sci.* 24, 191–224.
- Frausto da Silva, J.J.R., Williams, R.J.P., 2001. *The Biological Chemistry of the Elements*, 2nd ed. Oxford University Press, New York.
- Froelich, P.N., Klinkhammer, G.P., Bender, M.L., Luedtke, N.A., Heath, G.R., Cullen, D., Dauphin, P., Hammond, D., Hartman, B., Maynard, V., 1979. Early oxidation of organic matter in pelagic sediments of the eastern equatorial Atlantic: suboxic diagenesis. *Geochim. Cosmochim. Acta* 43, 1075–1090.
- Gaillardet, J., Viers, J., Dupre, B., 2003. 5.09 trace elements in river waters. In: Drever, J.I. (Ed.), *Surface and Ground Water, Weathering, and Soils*. Elsevier, pp. 225–272.
- German, C.R., Campbell, A.C., Edmond, J.M., 1991. Hydrothermal scavenging at the Mid-Atlantic Ridge: Modification of trace element dissolved fluxes. *Earth Planet. Sci. Lett.* 107, 101–114.
- Glassley, W.E., Piper, D.Z., 1978. Cobalt and scandium partitioning versus iron content for crystalline phases in ultramafic nodules. *Earth Planet. Sci. Lett.* 39, 173–178.
- Gunnarsson, M., Jakobsson, A.-M., Ekberg, S., Albinsson, Y., Ahlberg, E., 2000. Sorption studies of Cobalt(II) on colloidal hematite using potentiometry and radioactive tracer technique. *J. Colloid Interface Sci.* 231, 326–336.
- Helliwell, K.E., Wheeler, G.L., Leptos, K.C., Goldstein, R.E., Smith, A.G., 2011. Insights into the evolution of vitamin B12 auxotrophy from sequenced algal genomes. *Mol. Biol. Evol.* 28, 2921–2933.
- Helz, G.R., Bura-Nakić, E., Mikac, N., Ciglenečki, I., 2011. New model for molybdenum behavior in euxinic waters. *Chem. Geol.* 284, 323–332.
- Hetzl, A., Böttcher, M.E., Wortmann, U.G., Brumsack, H.-J., 2009. Paleo-redox conditions during OAE 2 reflected in Demerara Rise sediment geochemistry (ODP Leg 207). *Palaeogeogr. Palaeoclimatol. Palaeoecol.* 273, 302–328.
- Ho, T.-Y., Quigg, A., Finkel, Z.V., Milligan, A.J., Wyman, K., Falkowski, P.G., Morel, F.M.M., 2003. The elemental composition of some marine phytoplankton. *J. Phycol.* 39, 1145–1159.
- Hrshceva, E., Scott, S.D., 2007. Geochemistry and morphology of metalliferous sediments and oxyhydroxides from the Endeavour segment, Juan de Fuca Ridge. *Geochim. Cosmochim. Acta* 71, 3476–3497.
- Huerta-Diaz, M.A., Morse, J.W., 1992. Pyritization of trace metals in anoxic marine sediments. *Geochim. Cosmochim. Acta* 56, 2681–2702.
- Isley, A.E., 1995. Hydrothermal plumes and the delivery of iron to banded iron formations. *J. Geol.* 103, 169–185.
- Kamber, B.S., 2010. Archean mafic-ultramafic volcanic landmasses and their effect on ocean-atmosphere chemistry. *Chem. Geol.* 274, 19–28.
- Kamber, B.S., Greig, A., Collerson, K.D., 2005. A new estimate for the composition of weathered young upper continental crust from alluvial sediments, Queensland, Australia. *Geochim. Cosmochim. Acta* 69, 1041–1058.
- Knoll, A.H., Summons, R.E., Waldbauer, J.R., Zumberge, J.E., 2007. The geological succession of primary producers in the oceans. In: Falkowski, P.G., Knoll, A.H. (Eds.), *Evolution of Primary Producers in the Sea*. Elsevier, Boston, pp. 133–163.
- Konhauser, K.O., Newman, D.K., Kappler, A., 2005. The potential significance of microbial Fe(III) reduction during deposition of Precambrian banded iron formations. *Geobiology* 3, 167–177.
- Konhauser, K.O., Lalonde, S.V., Amskold, L., Holland, H.D., 2007. Was there really an Archean phosphate crisis?. *Science* 315, 1234.
- Konhauser, K.O., Pecoits, E., Lalonde, S.V., Papineau, D., Nisbet, E.G., Barley, M.E., Arndt, N.T., Zahnle, K., Kamber, B.S., 2009. Oceanic nickel depletion and a methanogen famine before the Great Oxidation Event. *Nature* 458, 750–753.
- Konhauser, K.O., Lalonde, S.V., Planavsky, N.J., Pecoits, E., Lyons, T.W., Mojzsis, S.J., Rouxel, O.J., Barley, M.E., Rosiere, C., Fralick, P.W., Kump, L.R., Bekker, A., 2011. Aerobic bacterial pyrite oxidation and acid rock drainage during the Great Oxidation Event. *Nature* 478, 369–373.
- Koschinsky, A., Hein, J.R., 2003. Uptake of elements from seawater by ferromanganese crusts: solid-phase associations and seawater speciation. *Mar. Geol.* 198, 331–351.
- Krauskopf, K.B., 1956. Factors controlling the concentrations of thirteen rare metals in sea-water. *Geochim. Cosmochim. Acta* 9, 1–32.
- Kremling, K., 1983. The behavior of Zn, Cd, Cu, Ni, Co, Fe, and Mn in anoxic baltic waters. *Mar. Chem.* 13, 87–108.
- Krishnaswami, S., 1976. Authigenic transition elements in Pacific pelagic clays. *Geochim. Cosmochim. Acta* 40, 425–434.
- Limpert, E., Stahel, W.A., Abbt, M., 2001. Log-normal distributions across the sciences: keys and clues. *Bioscience* 51, 341–352.
- Lyons, T.W., Werne, J.P., Hollander, D.J., Murray, R.W., 2003. Contrasting sulfur geochemistry and Fe/Al and Mo/Al ratios across the last oxic-to-anoxic transition in the Cariaco Basin, Venezuela. *Chem. Geol.* 195, 131–157.
- Manceau, A., Drits, V.A., Silvester, E., Bartoli, C., Lanson, B., 1997. Structural mechanism of Co<sup>2+</sup> oxidation by the phyllo-manganate buserite. *Am. Mineral.* 82, 1150–1175.
- Metz, S., Trefry, J.H., 2000. Chemical and mineralogical influences on concentrations of trace metals in hydrothermal fluids. *Geochim. Cosmochim. Acta* 64, 2267–2279.
- Moffett, J.W., Ho, J., 1996. Oxidation of cobalt and manganese in seawater via a common microbially catalyzed pathway. *Geochim. Cosmochim. Acta* 60, 3415–3424.
- Morel, F.M.M., Reinfelder, J.R., Roberts, S.B., Chamberlain, C.P., Lee, J.G., Yee, D., 1994. Zinc and carbon co-limitation of marine phytoplankton. *Nature* 369, 740–742.
- Morse, J.W., Arakaki, T., 1993. Adsorption and coprecipitation of divalent metals with mackinawite (FeS). *Geochim. Cosmochim. Acta* 57, 3635–3640.
- Morse, J.W., Luther III, G.W., 1999. Chemical influences on trace metal-sulfide interactions in anoxic sediments. *Geochim. Cosmochim. Acta* 63, 3373–3378.
- Murray, J.W., Dillard, J.G., 1979. The oxidation of cobalt(II) adsorbed on manganese dioxide. *Geochim. Cosmochim. Acta* 43, 781–787.
- Murray, K.J., Webb, S.M., Bargar, J.R., Tebo, B.M., 2007. Indirect oxidation of Co(II) in the presence of the marine Mn(II)-oxidizing bacterium *Bacillus* sp. strain SG-1. *Appl. Environ. Microbiol.* 73, 6905–6909.
- Musić, S., Gessner, M., Wolf, R.H.H., 1979. Sorption of small amounts of cobalt(II) on iron(III) oxide. *Mikrochim. Acta* 71, 105–112.
- Nisbet, E.G., Fowler, C.M.R., 1996. The hydrothermal imprint on life: did heat-shock proteins, metalloproteins and photosynthesis begin around hydrothermal vents?. *Geol. Soc. (Lond.) Spec. Publ.* 118, 239–251.
- Noble, A.E., Saito, M.A., Maiti, K., Benitez-Nelson, C.R., 2008. Cobalt, manganese, and iron near the Hawaiian Islands: A potential concentrating mechanism for cobalt within a cyclonic eddy and implications for the hybrid-type trace metals. *Deep-Sea Res., Part 2, Top. Stud. Oceanogr.* 55, 1473–1490.
- Noble, A.E., Lamborg, C.H., Ohnemos, D.C., Lam, P.J., Goepfert, T.J., Measures, C.I., Frame, C.H., Casciotti, K.L., DiTullio, G.R., Jennings, J., Saito, M.A., 2012. Basin-scale inputs of cobalt, iron, and manganese from the Benguela-Angola front to the South Atlantic Ocean. *Limnol. Oceanogr.* 57, 989–1010.
- Orth, C.J., Attrep Jr., M., Quintana, L.R., Elder, W.P., Kauffman, E.G., Diner, R., Villamil, T., 1993. Elemental abundance anomalies in the late Cenomanian extinction interval: a search for the source(s). *Earth Planet. Sci. Lett.* 117, 189–204.
- Öztürk, M., 1995. Trends of trace metal (Mn, Fe, Co, Ni, Cu, Zn, Cd and Pb) distributions at the oxic-anoxic interface in sulfidic water of the Drammensjord. *Mar. Chem.* 48, 329–342.
- Peng, P., Bleeker, W., Ernst, R.E., Söderlund, U., McNicoll, V., 2011. U–Pb baddeleyite ages, distribution and geochemistry of 925 Ma mafic dykes and 900 Ma sills in the North China craton: Evidence for a Neoproterozoic mantle plume. *Lithos* 127, 210–221.
- Piper, D.Z., Dean, W.E., 2002. Trace element deposition in the Cariaco Basin, Venezuela shelf, under sulfate-reducing conditions – a history of the local hydrography and global climate, 20 ka to the present. *USGS Professional Paper*. 45 pp.
- Planavsky, N.J., Rouxel, O.J., Bekker, A., Lalonde, S.V., Konhauser, K.O., Reinhard, C.T., Lyons, T.W., 2010. The evolution of the marine phosphate reservoir. *Nature* 467, 1088–1090.
- Planavsky, N.J., McGoldrick, P., Scott, C.T., Li, C., Reinhard, C.T., Kelly, A.E., Chu, X., Bekker, A., Love, G.D., Lyons, T.W., 2011. Widespread iron-rich conditions in the mid-Proterozoic ocean. *Nature* 477, 448–451.
- Pons, M.L., Fujii, T., Rosing, M., Quitté, G., Télouk, P., Albarède, F., 2013. A Zn isotope perspective on the rise of continents. *Geobiology* 11, 201–214.
- Poulton, S.W., Fralick, P.W., Canfield, D.E., 2004. The transition to a sulphidic ocean ~1.84 billion years ago. *Nature* 431, 173–177.
- Rasmussen, B., Buick, R., 1999. Redox state of the Archean atmosphere: Evidence from detrital heavy minerals in ca. 3250–2750 Ma sandstones from the Pilbara Craton, Australia. *Geology* 27, 115–118.
- Rasmussen, B., Fletcher, I.R., Bekker, A., Muhling, J.R., Gregory, C.J., Thorne, A.M., 2012. Deposition of 1.88-billion-year-old iron formations as a consequence of rapid crustal growth. *Nature* 484, 498–501.
- Reinhard, C.T., Planavsky, N.J., Robbins, L.J., Partin, C.A., Gill, B.C., Lalonde, S.V., Bekker, A., Konhauser, K.O., Lyons, T.W., 2013. Proterozoic ocean redox and biogeochemical stasis. *Proc. Natl. Acad. Sci. USA*.
- Robbins, L.J., Lalonde, S.V., Saito, M.A., Planavsky, N.J., Mloszewski, A.M., Pecoits, E., Scott, C., Dupont, C.L., Kappler, A., Konhauser, K.O., 2013. Authigenic iron oxide proxies for marine zinc over geological time and implications for marine eukaryotic metallome evolution. *Geobiology* 11, 295–306.
- Rouxel, O.J., Bekker, A., Edwards, K.J., 2005. Iron isotope constraints on the Archean and Paleoproterozoic ocean redox state. *Science* 307, 1088–1091.
- Rouxel, O.J., Bekker, A., Edwards, K.J., 2006. Response to comment on “Iron isotope constraints on the Archean and Paleoproterozoic ocean redox state. *Science* 311.
- Sahoo, S.K., Planavsky, N.J., Kendall, B., Wang, X., Shi, X., Scott, C., Anbar, A.D., Lyons, T.W., Jiang, G., 2012. Ocean oxygenation in the wake of the Marinoan glaciation. *Nature* 489, 546–549.
- Saito, M.A., Goepfert, T.J., 2008. Zinc-cobalt colimitation of *Phaeocystis antarctica*. *Limnol. Oceanogr.* 53, 266–275.
- Saito, M.A., Moffett, J.W., 2001. Complexation of cobalt by natural organic ligands in the Sargasso Sea as determined by a new high-sensitivity electrochemical cobalt speciation method suitable for open ocean work. *Mar. Chem.* 75, 49–68.

- Saito, M.A., Moffett, J.W., 2002. Temporal and spatial variability of cobalt in the Atlantic Ocean. *Geochim. Cosmochim. Acta* 66, 1943–1953.
- Saito, M.A., Moffett, J.W., Chisholm, S.W., Waterbury, J.B., 2002. Cobalt limitation and uptake in *Prochlorococcus*. *Limnol. Oceanogr.* 47, 1629–1636.
- Saito, M.A., Sigman, D.M., Morel, F.M.M., 2003. The bioinorganic chemistry of the ancient ocean: the co-evolution of the cyanobacterial metal requirements and biogeochemical cycles at the Archean–Paleoproterozoic boundary?. *Inorg. Chim. Acta* 356, 308–318.
- Saito, M.A., Moffett, J.W., DiTullio, G.R., 2004. Cobalt and nickel in the Peru upwelling region: A major flux of labile cobalt utilized as a micronutrient. *Glob. Biogeochem. Cycles* 18, GB4030.
- Saito, M.A., Rocap, G., Moffett, J.W., 2005. Production of cobalt binding ligands in a *Synechococcus* feature at the Costa Rica upwelling dome. *Limnol. Oceanogr.* 50, 279–290.
- Saito, M.A., Goepfer, T.J., Noble, A.E., Bertrand, E.M., Sedwick, P.N., DiTullio, G.R., 2010. A seasonal study of dissolved cobalt in the Ross Sea, Antarctica: micronutrient behavior, absence of scavenging, and relationships with Zn, Cd, and P. *Biogeochemistry* 7, 4059–4082.
- Saito, M.A., Bertrand, E.M., Dutkiewicz, S., Bulygin, V.V., Moran, D.M., Monteiro, F.M., Follows, M.J., Valois, F.W., Waterbury, J.B., 2011. Iron conservation by reduction of metalloenzyme inventories in the marine diazotroph *Crocosphaera watsonii*. *Proc. Natl. Acad. Sci. USA* 108, 2184–2189.
- Saito, M.A., Noble, A.E., Tagliabue, A., Goepfert, T.J., Lamborg, C.H., Jenkins, W.J., 2013. Slow-spreading submarine ridges in the South Atlantic as a significant oceanic iron source. *Nat. Geosci.* 6, 775–779.
- Sander, S.G., Koschinsky, A., 2011. Metal flux from hydrothermal vents increased by organic complexation. *Nat. Geosci.* 4, 145–150.
- Scott, C., Lyons, T.W., 2012. Contrasting molybdenum cycling and isotopic properties in euxinic versus non-euxinic sediments and sedimentary rocks: Refining the paleoproxies. *Chem. Geol.* 324–325, 19–27.
- Scott, C., Lyons, T.W., Bekker, A., Shen, Y., Poulton, S.W., Chu, X., Anbar, A.D., 2008. Tracing the stepwise oxygenation of the Proterozoic ocean. *Nature* 452, 456–459.
- Scott, C., Planavsky, N.J., Dupont, C.L., Kendall, B., Gill, B.C., Robbins, L.J., Husband, K.F., Arnold, G.L., Wing, B.A., Poulton, S.W., Bekker, A., Anbar, A.D., Konhauser, K.O., Lyons, T.W., 2012. Bioavailability of zinc in marine systems through time. *Nat. Geosci.* 6, 125–128.
- Shelley, R.U., Sedwick, P.N., Bibby, T.S., Cabedo-Sanz, P., Church, T.M., Johnson, R.J., Macey, A.I., Marsay, C.M., Sholkovitz, E.R., Ussher, S.J., Worsfold, P.J., Lohan, M.C., 2012. Controls on dissolved cobalt in surface waters of the Sargasso Sea: Comparisons with iron and aluminum. *Glob. Biogeochem. Cycles* 26.
- Snow, L.J., Duncan, R.A., Bralower, T.J., 2005. Trace element abundances in the Rock Canyon Anticline, Pueblo, Colorado, marine sedimentary section and their relationship to Caribbean plateau construction and oxygen anoxic event 2. *Paleoceanography* 20, PA3005.
- Stockdale, A., Davison, W., Zhang, H., Hamilton-Taylor, J., 2010. The association of cobalt with iron and manganese (oxyhydr)oxides in marine sediment. *Aquat. Geochem.* 16, 575–585.
- Stramma, L., Johnson, G.C., Sprintall, J., Mohrholz, V., 2008. Expanding oxygen-minimum zones in the tropical oceans. *Science* 320, 655–658.
- Sunda, W.G., Huntsman, S.A., 1995. Cobalt and zinc interreplacement in marine phytoplankton: biological and geochemical implications. *Limnol. Oceanogr.* 40, 1404–1417.
- Tagliabue, A., Bopp, L., Dutay, J.-C., Bowie, A.R., Chever, F., Jean-Baptiste, P., Bucciarelli, E., Lannuzel, D., Remenyi, T., Sarthou, G., Aumont, O., Gehlen, M., Jeandel, C., 2010. Hydrothermal contribution to the oceanic dissolved iron inventory. *Nat. Geosci.* 3, 252–256.
- Takahashi, Y., Manceau, A., Geoffroy, N., Marcus, M.A., Usui, A., 2007. Chemical and structural control of the partitioning of Co, Ce, and Pb in marine ferromanganese oxides. *Geochim. Cosmochim. Acta* 71, 984–1008.
- Toner, B.M., Fakra, S.C., Manganini, S.J., Santelli, C.M., Marcus, M.A., Moffett, J.W., Rouxel, O., German, C.R., Edwards, K.J., 2009. Preservation of iron(II) by carbon-rich matrices in a hydrothermal plume. *Nat. Geosci.* 2, 197–201.
- Turgeon, S.C., Creaser, R.A., 2008. Cretaceous oceanic anoxic event 2 triggered by a massive magmatic episode. *Nature* 454, 323–326.
- van der Weijden, C.H., 2002. Pitfalls of normalization of marine geochemical data using a common divisor. *Mar. Geol.* 184, 167–187.
- van der Weijden, C.H., Reichart, G.-J., van Os, B.J.H., 2006. Sedimentary trace element records over the last 200 kyr from within and below the northern Arabian Sea oxygen minimum zone. *Mar. Geol.* 231, 69–88.
- Veizer, J., Compston, W., Clauer, N., Schidlowski, M., 1983. <sup>87</sup>Sr/<sup>86</sup>Sr in Late Proterozoic carbonates: evidence for a “mantle” event at ~900 Ma ago. *Geochim. Cosmochim. Acta* 47, 295–302.
- Viollier, E., Jézéquel, D., Michard, G., Pèpe, M., Sarazin, G., Albéric, P., 1995. Geochemical study of a crater lake (Pavin Lake, France): trace-element behaviour in the monimolimnion. *Chem. Geol.* 125, 61–72.
- Wedephol, K.H., 1971. Environmental influences on the chemical composition of shales and clays. In: Ahrens, L.H., Press, F., Runcorn, S.K., Urey, H.C. (Eds.), *Physics and Chemistry of the Earth*. Pergamon Press, Oxford, United Kingdom, pp. 307–333.
- Wheat, C.G., Jannasch, H.W., Kastner, M., Plant, J.N., DeCarlo, E.H., 2003. Seawater transport and reaction in upper oceanic basaltic basement: chemical data from continuous monitoring of sealed boreholes in a ridge flank environment. *Earth Planet. Sci. Lett.* 216, 549–564.
- Yee, N., Fein, J.B., 2003. Quantifying metal adsorption onto bacteria mixtures: a test and application of the surface complexation model. *Geomicrobiol. J.* 20, 43.
- Yucel, M., Gartman, A., Chan, C.S., Luther, G.W., 2011. Hydrothermal vents as a kinetically stable source of iron-sulphide-bearing nanoparticles to the ocean. *Nat. Geosci.* 4, 367–371.
- Zerkle, A.L., House, C.H., Brantley, S.L., 2005. Biogeochemical signatures through time as inferred from whole microbial genomes. *Am. J. Sci.* 305, 467–502.
- Zhang, Y., Gladyshev, V.N., 2010. General trends in trace element utilization revealed by comparative genomic analyses of Co, Cu, Mo, Ni, and Se. *J. Biol. Chem.* 285, 3393–3405.